

# An Experimental and Theoretical Investigation of Loperamide Hydrochloride–Glutaric Acid Cocrystals

Giovanna Bruni,<sup>\*,†</sup> Mariarosia Maietta,<sup>†</sup> Laurotta Maggi,<sup>‡</sup> Piercarlo Mustarelli,<sup>†</sup> Chiara Ferrara,<sup>†</sup> Vittorio Berbenni,<sup>†</sup> Mauro Freccero,<sup>§</sup> Federico Scotti,<sup>†</sup> Chiara Milanese,<sup>†</sup> Alessandro Girella,<sup>†</sup> and Amedeo Marini<sup>†</sup>

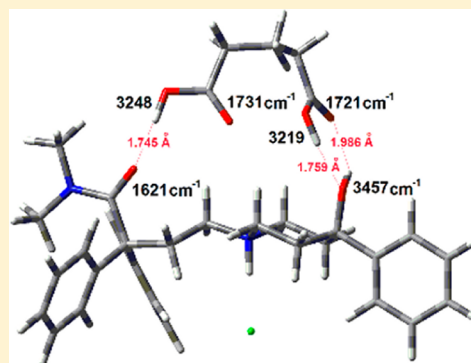
<sup>†</sup>C.S.G.I. - Department of Chemistry, Physical-Chemistry Section, University of Pavia, Viale Taramelli 16, 27100 Pavia, Italy

<sup>‡</sup>Department of Drug Sciences, University of Pavia, Viale Taramelli 12, 27100 Pavia, Italy

<sup>§</sup>Department of Chemistry, Organic Chemistry Section, University of Pavia, Viale Taramelli 10, 27100 Pavia, Italy

## S Supporting Information

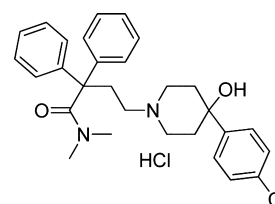
**ABSTRACT:** Cocrystallization is a powerful method to improve the physicochemical properties of drugs. Loperamide hydrochloride is a topical analgesic for the gastrointestinal tract showing low and pH-dependent solubility; for this reason, an enhancement of its solubility or dissolution rate, particularly at the pH of the intestinal tract, could improve its local efficacy. Here we prepared cocrystals of this active principle with glutaric acid and so obtained a new crystalline solid representing a viable alternative to improve the physicochemical properties and thus the pharmaceutical behavior of the drug. Differential scanning calorimetry, X-ray powder diffraction, Fourier infrared spectroscopy, solid-state NMR, and scanning electron microscopy coupled to the energy-dispersive X-ray spectrometry were used to investigate the new solid-phase formation. DFT calculations at B3LYP/6-31G(d) level of theory, in the gas phase, including frequencies computation, provided a rationale for the interaction between loperamide hydrochloride and glutaric acid. The cocrystals showed improved water solubility in comparison with loperamide HCl, and the pharmaceutical formulation proposed was able to release the drug more rapidly in comparison with three reference commercial products when tested at neutral pH values.



## 1. INTRODUCTION

Cocrystallization is a successful strategy to improve water solubility, which is a well-known obstacle to the drug development. Pharmaceutical cocrystals are formed between a drug and a coformer, both solid under ambient conditions, which interact by hydrogen bonds or other noncovalent and nonionic interactions.<sup>1–7</sup> As a consequence of a different crystal packing of the drug in the multicomponent system, a change of properties such as melting point, stability, solubility, and dissolution rate is achieved, while the pharmacologic activity of the drug is maintained. Because the hydrogen bond is the favorite interaction, the crystal formation can be rationalized considering the presence of hydrogen bonds donors and acceptors in the components molecules. The functional groups, such as carboxylic acids, amides, alcohols, and heterocyclic basis, are able to generate strong and directional hydrogen bonds. The presence of these functional groups is frequent in the structure of many active principles and, in addition to the biologic activity, it gives them also a great capability to generate supramolecular structures. The preparation and the physicochemical characterization of loperamide hydrochloride cocrystals is the subject of this manuscript. Loperamide hydrochloride [4-(4-chlorophenyl)-4-hydroxy-*N,N*-dimethyl-diphenyl-1-piperidine butanamide hydrochloride] is an antidiarrheal agent (Scheme 1). It is an opioid-receptor

## Scheme 1. Chemical Structure of Loperamide Hydrochloride



agonist and has direct antisecretory effect on myentericopiate receptors of the large intestine. Loperamide has minimal systemic availability (0.3%), with most of the drug being removed by first-pass metabolism, which further supports a local action in the gut.<sup>8</sup> Loperamide hydrochloride is considered a class-IV molecule (low solubility–low permeability) in the Biopharmaceutics Classification Scheme (BCS);<sup>9</sup> it shows pH-dependent solubility: higher in acidic environment and lower at neutral pH (fed state). However, because of its local action, an enhancement of its solubility at neutral pH could improve drug disposition at the site of action and the therapeutic effect, independent of the

Received: April 30, 2013

Revised: June 13, 2013

Published: June 13, 2013



environmental pH. It has a long acting effect; however, its maximum therapeutic impact may not manifest for 16–24 h, and this has implication for initial dosing.<sup>10</sup> Because this drug is only slightly water-soluble, it is a good candidate for the cocrystals formation.<sup>11</sup> A cocrystal screening process with several coformers (4-amino benzoic acid, benzoic acid, fumaric acid, glutaric acid, sorbic acid, succinic acid, L-tartaric acid, niacinamide, and saccharine) was performed. A certain formation of cocrystals was found only using glutaric acid as the coformer. Differential scanning calorimetry (DSC), X-ray powder diffraction (XRPD), Fourier infrared spectroscopy (FT-IR), solid-state NMR (SSNMR) and scanning electron microscopy coupled to the energy-dispersive X-ray spectrometry (SEM-EDS)<sup>3,12</sup> were used as analytical tools to identify and physicochemically characterize the obtained solid phases. While DSC, XRPD, and FT-IR are the techniques traditionally used for verifying the cocrystal formation, SSNMR has been rarely used in the characterization of cocrystals and even more rarely SEM-EDS. However, the SSNMR is a suitable technique to this aim because it is non-destructive, can study small amounts of powder, and is sensitive to hydrogen bonds and local conformational changes. Moreover, the possibility to use different 1-D and 2-D pulse sequences and to investigate different nuclei (typically <sup>1</sup>H and <sup>13</sup>C) can help to obtain a detailed structural information about pharmaceutical cocrystals.<sup>13</sup> <sup>1</sup>H and <sup>13</sup>C SSNMR were used to address the weak interactions at the basis of the cocrystal. Moreover, DFT calculations at the B3LYP/6-31G(d) level of theory, in the gas phase, including frequencies computation, provided a rationale for the interaction between loperamide hydrochloride and glutaric acid. The new phase obtained was further characterized in terms of water solubility and dissolution rate enhancement, in comparison with three commercial products at different pH values.

## 2. EXPERIMENTAL METHODS

**2.1. Materials.** Loperamide hydrochloride was kindly donated by Sifavitor S.r.l. (Italy). The coformers selected to prepare cocrystals were 4-amino benzoic acid, benzoic acid, fumaric acid, glutaric acid, sorbic acid, succinic acid, L-tartaric acid, niacinamide, and saccharine, all obtained from the Sigma-Aldrich Company (Milan, Italy). Among these molecules, only glutaric acid gave interesting results, and for this reason we will discuss only the loperamide hydrochloride–glutaric acid system.

The binary system (LGA11 in the following) was prepared through solvent evaporation: loperamide hydrochloride and the glutaric acid in 1:1 molar ratio were dissolved in hot ethanol under magnetic stirring. The clear solution was then let to cool spontaneously at ambient temperature, and the solvent was allowed to evaporate slowly until a solid sample was obtained.

For tablets production, LGA11 powder was used as such (Lop1 formulation) or sieved through a 36  $\mu$ m screen (Lop2 formulation) to test the effect of particle size on the dissolution rate. The proper amount of active principle (corresponding to 2.0 mg of drug dose) was mixed in a Turbula apparatus for 20 min with 100 mg of corn starch, 5.0 mg of talc, 3.0 mg of magnesium stearate (all from C. Erba, Milan, Italy), 50 mg of Crospovidone NF (Gaf Corporation, New York), and 20 mg of lactose monohydrate Tablettose 80 (Meggler AG, Wasserburg, Germany). Flat tablets of 8 mm in diameter were then prepared using a single punch tableting machine (Korsh EKO, Berlin, Germany). Three commercial products were used as references:

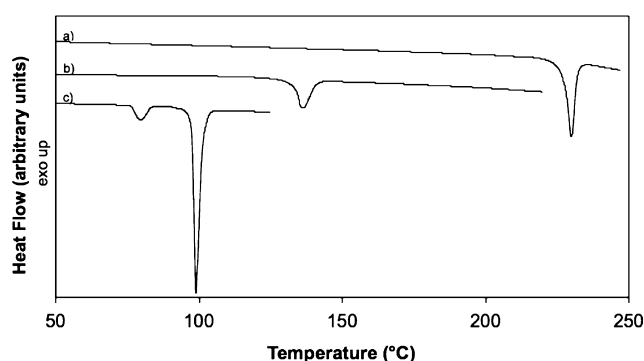


**Figure 1.** DSC curves of (a) loperamide hydrochloride, (b) LGA11, and (c) glutaric acid.

Imodium capsules (Johnson & Johnson S.p.A. Pomezia, Italy), Dissenten tablets (Società Prodotti Antibiotici S.p.A., Milan, Italy), and Loperamide DOC Generici tablets (DOC Generici S.r.l., Milan, Italy) all containing 2.0 mg of Loperamide hydrochloride.

**2.2. Instruments and Procedures.** **2.2.1. Thermal Analysis.** Thermal analyses were carried out using a TGA Q5000 IR apparatus and a DSC Q2000 apparatus both interfaced with a TA 5000 data station (TA Instruments, New Castle, DE). The DSC instrument was calibrated for temperature and enthalpy using ultrapure indium. Samples were scanned from 40 to 300 °C at 10 K·min<sup>-1</sup> in open standard aluminum pans under a continuously purged dry-nitrogen atmosphere (3 L·h<sup>-1</sup>). The data were collected in triplicate for each sample.

**2.2.2. Spectroscopic Techniques.** Fourier transform infrared spectra were recorded using a Nicolet FT-IR iS10 spectrometer (Nicolet, Madison, WI) equipped with ATR (attenuated total reflectance) sampling accessory (Smart iTR with ZnSe plate) by coadding 256 scans in the 4000–650 cm<sup>-1</sup> range at 4 cm<sup>-1</sup> resolution.

**2.2.3. X-ray Powder Diffraction.** XRPD measurements were performed using a D5005 Bruker diffractometer (Karlsruhe, Germany) (Cu K $\alpha$  radiation; voltage of 40 kV and current of 40 mA) equipped with a  $\theta$ – $\theta$  vertical goniometer and a position sensitive detector (PSD, Braun, Garching, Germany). The patterns were recorded at ambient temperature in a step scan mode (step size: 0.015°, counting time: 1.3 s·step<sup>-1</sup>) in the 5 < 2 $\theta$  < 35 angular range.

**2.2.4. Solid-State NMR.** The solid-state NMR spectra were acquired on a 400 MHz spectrometer (Avance III, Bruker, Karlsruhe, Germany) based on a wide-bore 9.4 T magnet equipped with a 4 mm MAS probe. <sup>1</sup>H spectra were acquired with a single-pulse sequence adopting a 90° pulse of 4  $\mu$ s, a delay time of 10 s, and by averaging over eight scans. <sup>13</sup>C spectra were acquired with <sup>1</sup>H–<sup>13</sup>C CPMAS. The <sup>1</sup>H 90° pulse was 4  $\mu$ s, the delay time was 30 s, the contact time was 2 ms, and the signals were averaged over 8k acquisitions for CP. The rotation frequency was 11 kHz for <sup>1</sup>H and 11 kHz for <sup>13</sup>C. Signals chemical shifts were referenced to TMS. The spectra were processed and analyzed with the package TOPSPIN (Bruker).

**2.2.5. Microscopic Analysis.** A Zeiss EVO MA10 (Carl Zeiss, Oberkochen, Germany) scanning electron microscope coupled to an EDS detector (X-max 50 mm<sup>2</sup>, Oxford Instruments, Oxford, United Kingdom) was used for the morphologic study and the elemental microanalysis of the

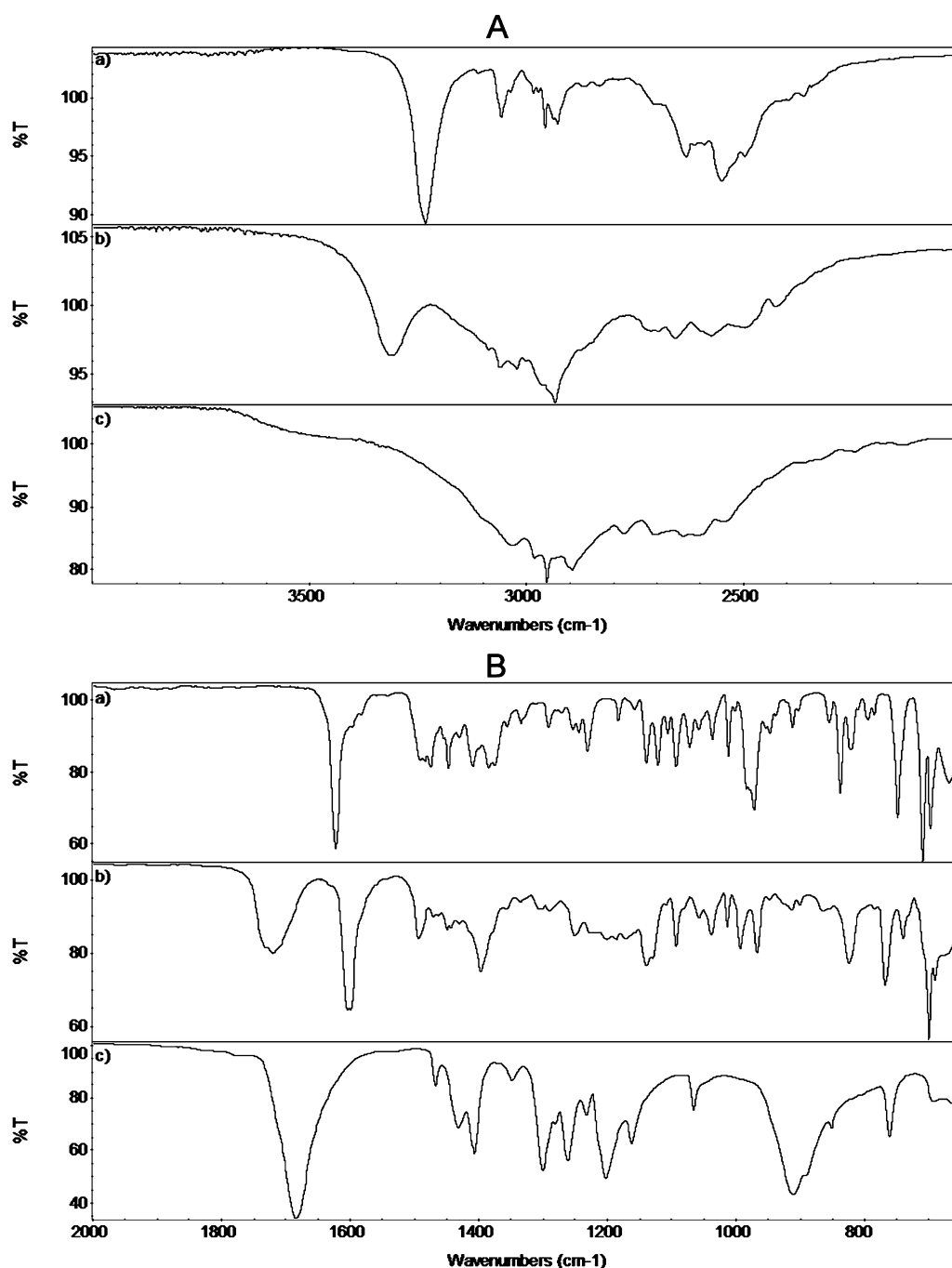


**Figure 2.** FT-IR spectra of: (a) loperamide hydrochloride, (b) *LGA11*, and (c) glutaric acid in the frequency region 4000–2000 cm<sup>-1</sup> (A) and 2000–650 cm<sup>-1</sup> (B).

samples. The observation was conducted on gold-sputtered samples.

**2.2.6. Solubility and Dissolution Rate Determination.** The solubility was determined in triplicate pouring an excess of drug in volumetric flasks (left under magnetic stirring, 300 rpm, for 2 h) at 21 °C in distilled water. Then, an aliquot of the liquid was filtered (0.45 μm, Millipore) and properly diluted and the concentration was determined by UV detection at 220 nm (Lambda 25 UV Winlab V6 software, Perkin-Elmer, Monza, Italy). The dissolution tests were performed using the USP Apparatus 2 (paddle, Erweka DT-D6, Dusseldorf, Germany), at 50 rpm, in 900 mL of deionized water (pH 6.8), 0.1 N hydrochloric acid pH 1.0, or phosphate buffer pH 7.2 at 37 °C.

The amount of drug released was determined by UV detection at 220 nm ( $n = 6$  repetitions).

**2.2.7. DFT Computational Details.** All calculations were carried out using the Gaussian 03 program package. All of the geometric structures of Loperamide hydrochloride (**1** and **2**, see Figure 6), Loperamide hydrochloride–formic acid 1:1 (**3** and **4**) taken as a model of an optimal H-bonding complex and the real Loperamide hydrochloride–glutaric acid complex (**5**) were fully optimized in the gas phase using the hybrid density functional method B3LYP with the 6-31G(d) basis set. To confirm the nature of the stationary points and to produce IR spectra, we calculated vibrational frequencies for all of the optimized structures. For the calculation of the harmonic

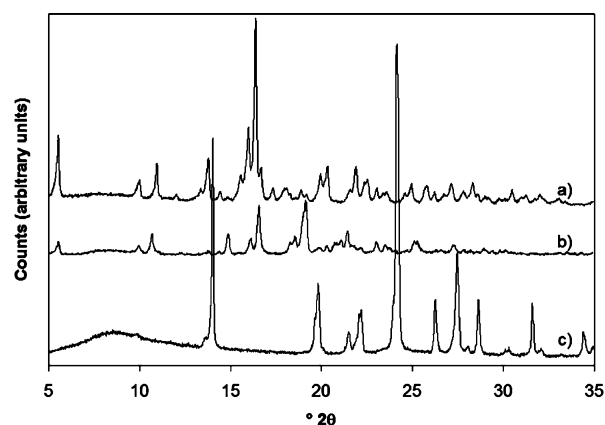


**Figure 3.** XRPD patterns of (a) loperamide hydrochloride, (b) *LGA11*, and (c) glutaric acid.

vibrational frequencies (in the harmonic approximation) with the B3LYP functional and 6-31G(d) basis sets, we considered the linear scaling factor of 0.9613, as suggested by Radom.<sup>14</sup>

### 3. RESULTS AND DISCUSSION

**3.1. Thermal Measurements.** The TGA analysis indicates that all of the samples are free of solvent.

DSC measurements were performed to compare the thermal behavior of the binary system *LGA11* with those of the pure components. Loperamide hydrochloride melts at  $T_{\text{onset}}$  227.4 °C (Figure 1, curve a) with enthalpy change ( $\Delta H$ ) of  $82.0 \pm 1.6 \text{ J}\cdot\text{g}^{-1}$ . The glutaric acid shows two peaks (Figure 1, curve c): the first one, at 76.6 °C ( $\Delta H = 17.6 \pm 1.1 \text{ J}\cdot\text{g}^{-1}$ ), is due to the transition of beta polymorph, the form stable at room temperature, to alpha polymorph; the second peak at 97.5 °C ( $\Delta H = 161.9 \pm 2.3 \text{ J}\cdot\text{g}^{-1}$ ) is the melting of alpha polymorph.<sup>15</sup> The DSC curve of the *LGA11* sample (Figure 1, curve b) is completely different from those of pure components. Indeed,

only a single endothermic peak is present at 133.3 °C ( $\Delta H = 48.8 \pm 1.9 \text{ J}\cdot\text{g}^{-1}$ ). It is beyond the thermal effects of glutaric acid and before the drug melting. So we can suppose that a new solid phase has formed as a consequence of cocrystallization.

**3.2. FT-IR.** The FT-IR technique can be used to confirm the cocrystal formation by evaluating the intermolecular interactions in consideration of the fact that the hydrogen-bond schemes are different in the various solid forms and that the peaks of the involved functional groups consequently shift to different frequencies.

The FT-IR spectrum of the *LGA11* system (Figure 2A,B, curve b) is considerably different from the simple superimposition of those of the pure components (Figure 2A,B, curves a and c). The main differences concern the following points:

- The peak due to O–H stretching of loperamide hydrochloride at  $3223 \text{ cm}^{-1}$  is now shifted to  $3311 \text{ cm}^{-1}$ .
- The peak due to C=O stretching of glutaric acid at  $1685 \text{ cm}^{-1}$  is shifted to  $1720 \text{ cm}^{-1}$ .
- The peak at  $1622 \text{ cm}^{-1}$  of C=O stretching of loperamide hydrochloride is shifted to  $1604 \text{ cm}^{-1}$ .
- The in-plane bending of C–O–H of glutaric acid is shifted from  $1406$  to  $1396 \text{ cm}^{-1}$ .
- The C–O stretching of dimeric glutaric acid ( $1300$  and  $1431 \text{ cm}^{-1}$ ) disappears.
- The out-of-plane bending of O–H group of glutaric acid ( $910 \text{ cm}^{-1}$ ) disappears.
- The out-of-plane bending of aromatic C–H is shifted to low frequency.

These spectral evidence suggest the alteration of the hydrogen-bond schemes. The changes mainly involve the carboxylic group of the glutaric acid and the –OH, the C=O groups, and the aromatic rings of loperamide hydrochloride.

**3.3. X-ray Powder Diffraction.** The XRPD patterns of loperamide hydrochloride, glutaric acid, and *LGA11* samples are reported in Figure 3. In the *LGA11* pattern, the presence of

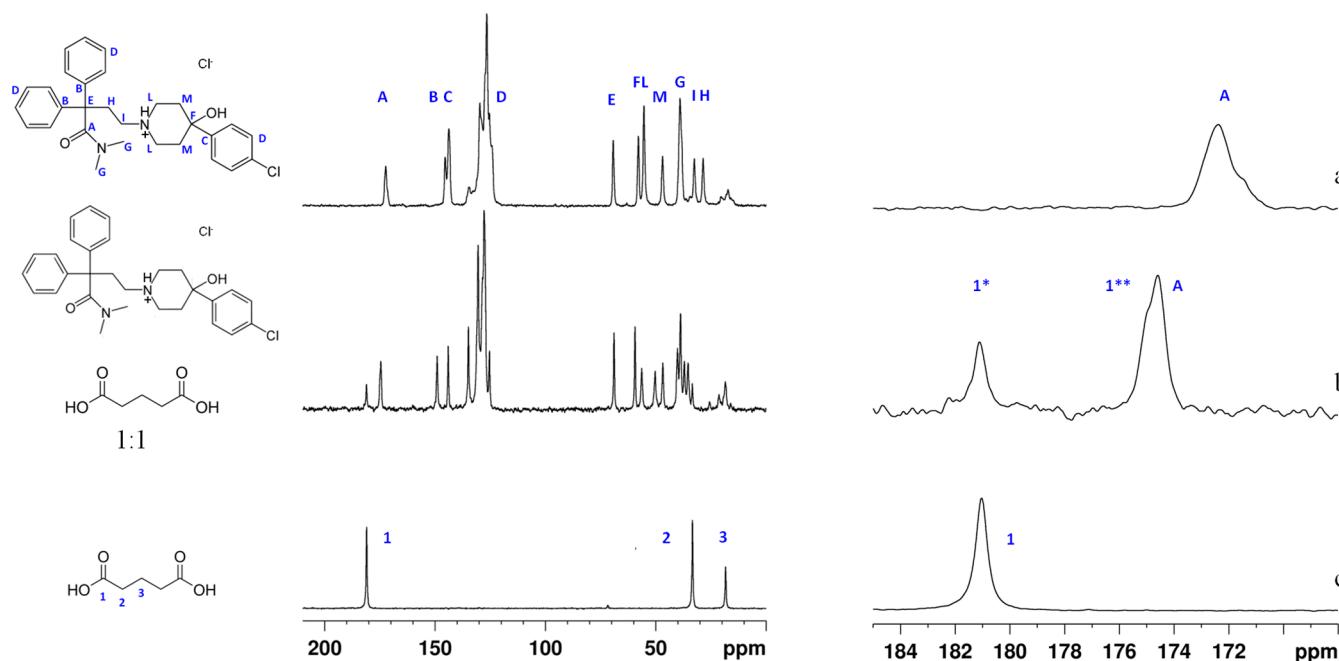


**Figure 4.**  $^{13}\text{C}$  spectra of loperamide hydrochloride (a), *LGA11* (b), and glutaric acid (c) recorded under MAS conditions with a CP sequence. # marks the sidebands; blue letters and numbers for the peaks assignment. In the frame, enlargement of the  $^{13}\text{C}$  spectra in the region 185–165 ppm.



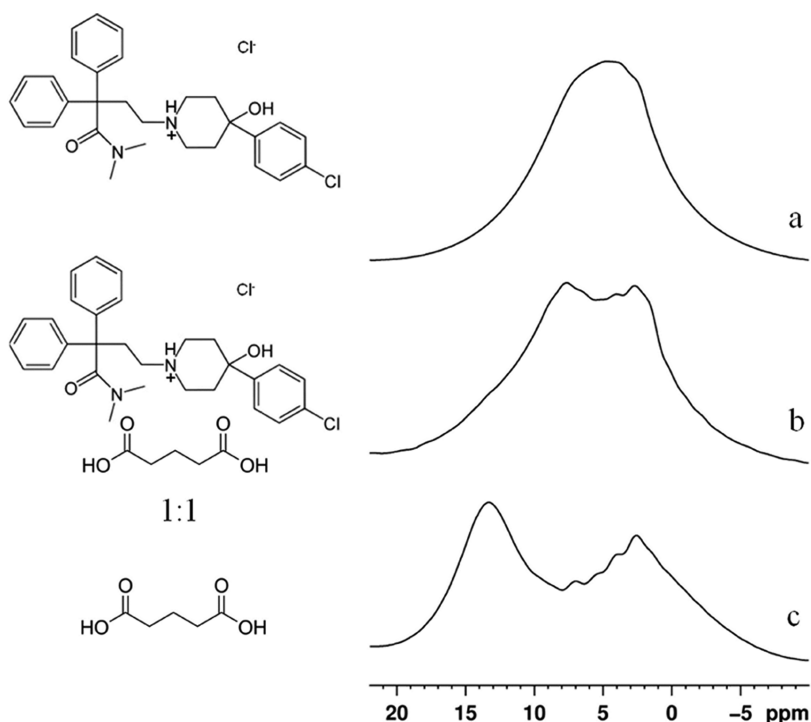


Figure 5.  $^1\text{H}$  spectra of loperamide hydrochloride (a), LGA11 (b), and glutaric acid (c).

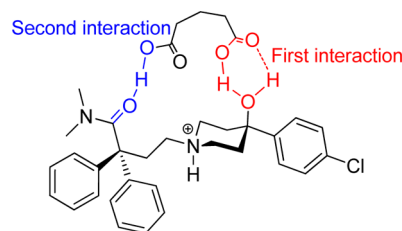
peaks at angular positions different from those typical of the pure components suggests the formation of a new solid phase.

**3.4. Solid-State NMR.** Figure 4 shows the  $^{13}\text{C}$  CP spectra of loperamide hydrochloride (a), LGA11 (b), and glutaric acid (c), together with the peaks assignment of the two starting molecules. Figure 5 shows the  $^1\text{H}$  SSNMR spectra of the same molecules. The  $^{13}\text{C}$  spectra clearly fulfill the first basic criterion for cocrystal formation, that is, that the spectrum of the cocrystal does not match the spectra of the starting materials. In particular, we focus our attention on the zoomed carbonyl region (see frame of Figure 4): the loperamide carbonyl is shifted  $\sim 2$  ppm downfield, whereas the one attributed to the glutaric acid seems to be split into two components, one of which is observed at the same chemical shift (181 ppm) and the other one at  $\sim 176$  ppm (seen as a shoulder of the loperamide carbonyl peak).

A careful analysis of the LGA11 spectrum suggests the existence of two different hydrogen-bonding interactions taking place between glutaric acid and loperamide hydrochloride molecules, in agreement with the DFT findings (see later).

The first interaction takes place between the carboxyl group of glutaric acid and the oxidryl group of loperamide. The carbonyl of glutaric acid plays the role of donor with respect to the acid proton of the loperamide hydroxyl group. At the same time, the oxygen atom of the loperamide hydroxyl group can act like a donor with respect to the acidic proton of the glutaric acid. (See Scheme 2.) This interaction is demonstrated by the following effects: the F peak is deshielded by  $\sim 1$  ppm, while signals M and C are deshielded by  $\sim 0.5$  ppm. These relatively small effects are indeed reasonable, if considering that the  $-\text{OH}$  group in pure loperamide is already involved in a relatively strong electrostatic interaction with  $\text{Cl}^-$  (see also DFT results). The  $\text{C}=\text{O}$  peak of glutaric acid (signal 1\*, at 181 ppm) is expected to be nearly unaffected with respect to that of the pure sample, which in turn is involved in a strong network of hydrogen bonds, as demonstrated by the 3 ppm shift downfield

**Scheme 2. Naïve Representation, Chiefly Based on the NMR Results, of the Interaction Motif between Glutaric Acid and Loperamide Hydrochloride in the Cocrystal Structure<sup>a</sup>**



<sup>a</sup>Loperamide "chair-like" conformational structure has been taken from ref 16, which reports a single-crystal study of pure loperamide hydrochloride.

with respect to glutaric acid in solution (178.5 ppm, SDDBS No.: 1094).

The second interaction takes place between the carbonyl oxygen (donor) of loperamide unit and the other  $-\text{OH}$  group (acceptor) of the glutaric acid with the formation of a hydrogen bond. This interaction is confirmed by the deshielding of the peak A ( $\sim 2$  ppm), assigned to the carbonyl group of the loperamide, and, to a lower extent ( $\sim 0.5$  ppm), of the peak E, which is attributed to the quaternary carbon. The carbonyl group of glutaric acid (peak 1\*\*) is strongly shielded (4 ppm) with respect to that of pure sample. This apparently strange result may be explained by considering that the formation of the cocrystal may break the complex hydrogen-bond network of pure glutaric acid.

$^1\text{H}$  spectra (Figure 5) are less informative because of the very large dipolar magnetic interaction, which is only partially removed by MAS rotation. However, a careful comparison of the spectra of glutaric acid and LGA11 allows us to infer that one of the  $-\text{OH}$  peaks is shifted upfield (i.e., more shielded) by 4 ppm in the cocrystal, in agreement with the hydrogen-bonding motif

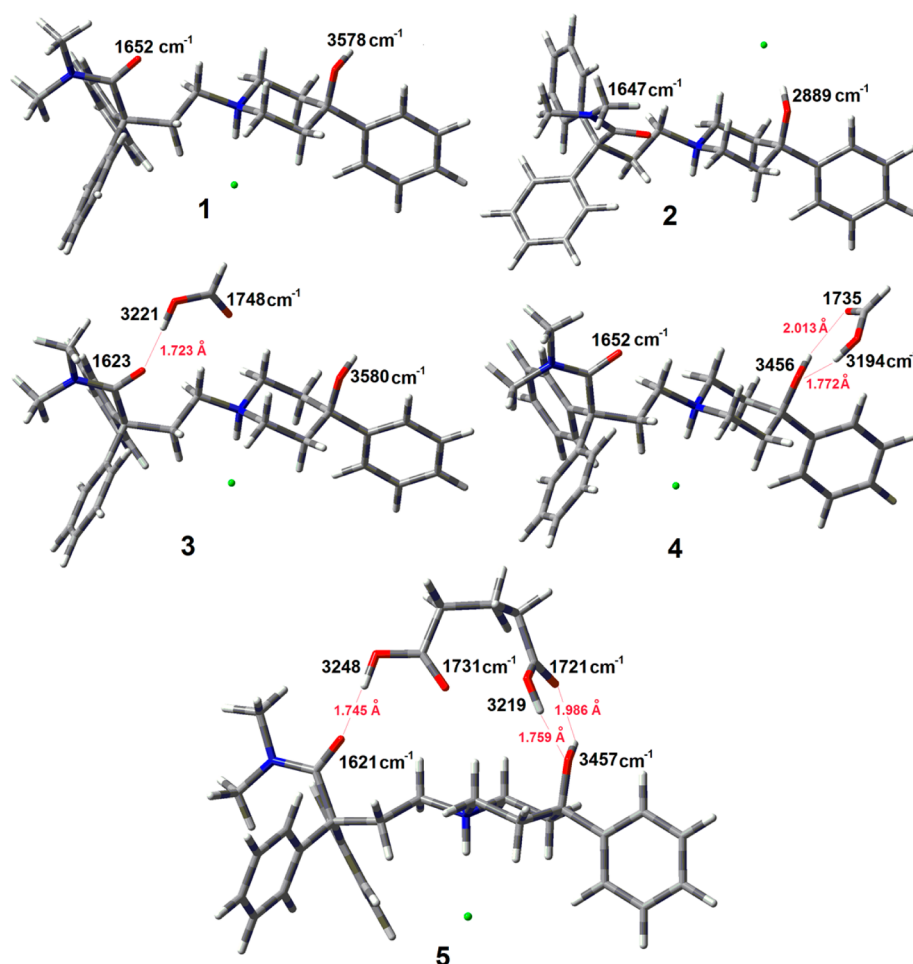


**Figure 6.** Geometries of loperamide hydrochloride exhibiting the chloride anion H-bonded to the cationic NH<sup>+</sup> (1) and the hydroxyl moieties (2), loperamide hydrochloride formic acid complexes 3 and 4, and loperamide hydrochloride–glutaric acid complex 5 optimized at the B3LYP/6-31G(d) level of theory in the gas phase. Frequency data (in cm<sup>-1</sup>) of the most important vibrational modes and key distances (in angstroms) between atoms involved in the H-bonding network are reported in black and in red, respectively.

sketched in Scheme 2. The presence of a shoulder at 12 ppm in Figure 5b suggests that the second –OH group of the glutaric acid is unaffected with respect to the pure sample, again in agreement with the above-mentioned scheme.

Our simple 1-D SSNMR approach demonstrates the formation of a new structure starting from glutaric acid and loperamide hydrochloride. The confirmation of the interactions motif as well as a more accurate information (e.g., hydrogen-bond lengths) does require the use of 2-D experiments (<sup>1</sup>H–<sup>13</sup>C CP-HETCOR, <sup>1</sup>H DQ-BABA).<sup>13</sup>

**3.5. DFT Calculations.** To simplify the calculation, we have replaced the *p*-Cl atom on the aromatic ring of Loperamide, being at long distance to the H-bonding moieties, by an H atom. The chairlike conformation of the piperidine ring has been taken into account because only a “chair-like” conformation has been reported from a single-crystal structure of pure loperamide hydrochloride.<sup>17</sup> The geometries of five different structures (1–5) have been optimized at the B3LYP/6-31G(d) level of theory in the gas phase (Figure 6). Two of them (1 and 2) describe the loperamide hydrochloride exhibiting the chloride anion H-bonded to the cationic NH<sup>+</sup> and the hydroxyl moieties, respectively. The loperamide hydrochloride–formic acid complexes 3 and 4 provide geometric and IR spectroscopic evidence of an optimal array characterized by the efficient H-bonding, involving the carboxylic group and both the

carboxamide (3) and hydroxyl moieties (4) of loperamide. Clearly, the loperamide hydrochloride–glutaric acid complex 5 exhibits a geometry where both glutaric acid carboxylic moieties are involved in a H-bonding network, which is similar, from a geometrical point of view, to those of the complexes 3 and 4. In addition, the similarity of the vibrational frequencies for the acidic hydrogens and carbonyl moieties in the complex 5 in comparison with those in 3 and 4 (see in detail Figure 6) further supports the evidence that glutaric acid can interact with both the carboxamide and hydroxyl moieties of loperamide hydrochloride without any substantial geometrical strain, as suggested by NMR data and sketched in Scheme 2. In fact, the H bonding between the acidic proton of glutaric acid and the carbonyl group of the carboxamide moiety (defined as “Second Interaction” in Scheme 2) exhibiting a 1.745 Å distance (very similar to 1.723 Å in the complex 3) is responsible for the reduced frequency of the carboxamide vibrational mode from 1652 to 1623 cm<sup>-1</sup> (see 3 in Figure 6), in agreement with the experimental IR data. The hydrogen-bonding network involving the second carboxylic group of glutaric acid, described as “first interaction” in the Scheme 2, should cause an increase in the loperamide–OH frequency, as such a frequency passes from 2889 cm<sup>-1</sup> in the complex 2 to 3456 cm<sup>-1</sup> in 5.

**3.6. SEM/EDS.** The powder of loperamide hydrochloride consists of irregular platelets of a few micrometers size often

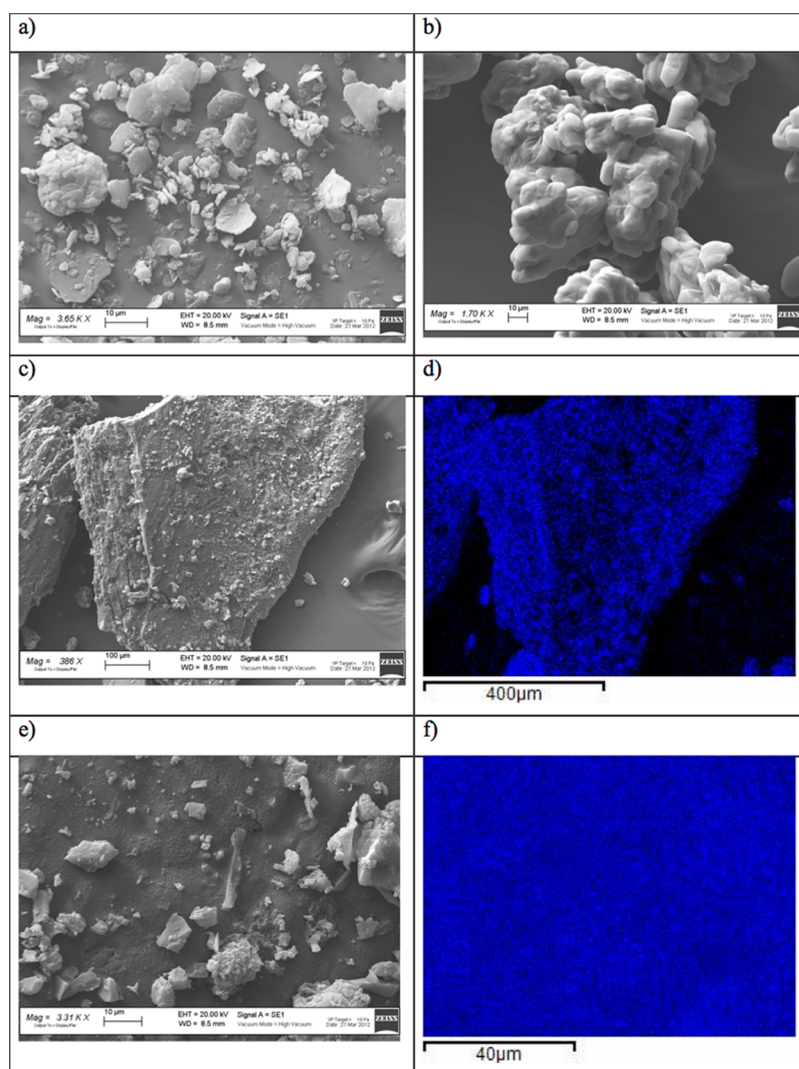


**Figure 7.** Microphotographs of loperamide (a), glutaric acid (b), *LGA11* (c,e), and chlorine map of *LGA11* (d,f).

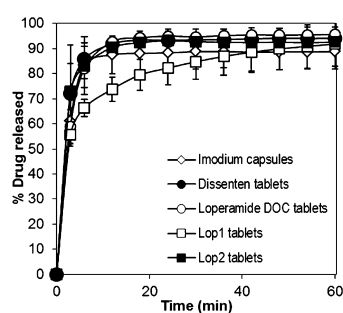


**Figure 8.** Dissolution profiles of the formulations tested in hydrochloric acid at pH 1.

aggregating together (Figure 7a). The coformer appears as irregular particle aggregates with size of several hundreds of micrometers (Figure 7b). The *LGA11* sample (Figure 7c) is made of particles with very irregular form and size, and it is not possible to recognize each component.

In our previous works,<sup>3,12</sup> the SEM-EDS technique has proved to be very useful and reliable in the characterization of multicomponent systems, and we performed also in this case the elemental microanalysis to confirm the hypothesis of the cocrystal formation. The map of chlorine, which is the element

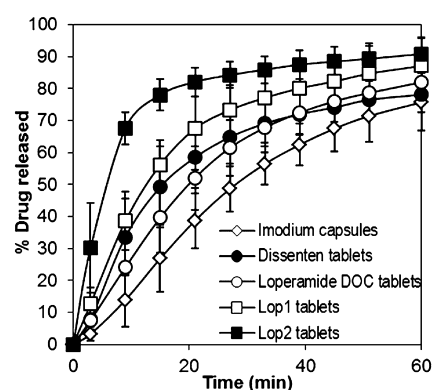


**Figure 9.** Dissolution profiles of the formulations tested in water.

present in the drug molecule but absent in that of the coformer, was recorded for the *LGA11* sample. In Figure 7d,f, the chlorine maps are reported, respectively, corresponding to the picture taken at 386X magnification (Figure 7c) and to the zoomed picture at 3310X magnification (Figure 7e). As it is evident in Figure 7c–f, the chlorine distribution is so uniform that the map accurately reproduces the sample morphology. This is another indication that the sample is not a simple

mixture of drug and coformer but that an interaction between the components has occurred, leading to the formation of cocrystals.

**3.7. Solubility and Dissolution Rate.** The loperamide hydrochloride solubility, measured in water at 21 °C, was  $10.1 \pm 1.4$  mg/100 mL, while *LGA11* solubility, under the same conditions, was increased to  $63.5 \pm 5.1$  mg/100 mL.

Because this drug is more soluble in an acidic environment, all of the formulations tested showed comparable dissolution behavior at pH 1; in fact, the dose is released completely in 10 min, except for *Lop1* formulation, containing *LGA11* powder of larger particle size, which just shows slightly slower rate of dissolution (Figure 8).

In contrast, when the dissolution test is performed in water (Figure 9), *Lop2* formulation showed the fastest dissolution profile, followed by *Lop1* and then by the commercial products. Under these conditions, both particle size fractions of the powder dissolved more rapidly than loperamide HCl, contained in the reference products, demonstrating that this faster dissolution rate is due only to the solubility behavior of the new *LGA11* phase. Even more different were the dissolution profiles obtained in phosphate buffer at pH 7.2, confirming that *LGA11* phase is able to dissolve more rapidly than loperamide HCl independently from the medium pH (Figure 10).

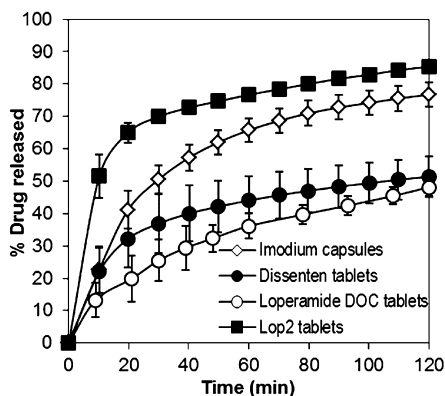


**Figure 10.** Dissolution profiles of the formulations tested in phosphate buffer pH 7.2.

#### 4. CONCLUSIONS

We reported the synthesis of a hydrogen-bonded supramolecular compound between loperamide hydrochloride and glutaric acid through solvent evaporation. Whereas the formation of the cocrystal could be simply inferred by comparing the thermograms and the NMR/FT-IR spectra of the starting materials with those of the final product, a deeper understanding of the chemical/physical interactions between the component molecules can be obtained by the combined use of spectroscopic and modeling approaches. Here the combination of spectroscopic techniques (FT-IR, SSNMR) and DFT calculations allowed us to obtain a clear insight into the complex hydrogen-bonding motifs, which are at the basis of the cocrystal formation.

The new solid phase shows six-fold increased solubility in water compared with loperamide HCl and a faster dissolution rate when formulated in tablets, in comparison with three reference commercial products, when tested at neutral pHs. This product could improve drug disposition for in vivo local

effect through the different environmental pHs of the gastrointestinal tract.

#### ■ ASSOCIATED CONTENT

##### Supporting Information

Table with Cartesian coordinates of the optimized models of Loperamide hydrochlorides **1** and **2**, Loperamide formic acid complexes **3** and **4**, and Loperamide hydrochloride–glutaric complex **5** at B3LYP/6-31G(d) level of theory. This material is available free of charge via the Internet at <http://pubs.acs.org>.

#### ■ AUTHOR INFORMATION

##### Corresponding Author

\*Tel: +39 0382 987667. Fax: +39 0382 987670. E-mail: [giovanna.bruni@unipv.it](mailto:giovanna.bruni@unipv.it).

##### Notes

The authors declare no competing financial interest.

#### ■ REFERENCES

- (1) Vishweshwar, P.; McMahon, J. A.; Bis, J. A.; Zaworoto, M. J. Pharmaceutical Co-crystals. *J. Pharm. Sci.* **2006**, *95*, 499–516.
- (2) Schulthesis, N.; Newman, A. Pharmaceutical Cocrystals and Their Physicochemical Properties. *Cryst. Growth Des.* **2009**, *9*, 2950–2967.
- (3) Bruni, G.; Maietta, M.; Berbenni, V.; Bini, M.; Ferrari, S.; Capsoni, D.; Boiocchi, M.; Milanese, C.; Marini, A. Preparation and Characterization of Carprofen Co-Crystals. *CrystEngComm* **2012**, *14*, 435–455.
- (4) Hockey, M. B.; Peterson, M. L.; Scoppettuolo, L. A.; Morrisette, S. L.; Vetter, A.; Guzman, H.; Remenar, J. F.; Zhang, Z.; Tawa, M. D.; Haley, S.; et al. Performance Comparison of a Co-Crystal of Carbamazepine with Marketed Product. *Eur. J. Pharm. Biopharm.* **2007**, *67*, 112–119.
- (5) Bak, A.; Gore, A.; Yanez, E.; Stanton, M.; Tufekcic, S.; Syed, R.; Akrami, A.; Rose, M.; Surapaneni, S.; Bostick, T.; et al. The Co-Crystal Approach to Improve the Exposure of a Water-Insoluble Compound: AMG 517 Sorbic Acid Co-Crystal Characterization and Pharmaceuticals. *J. Pharm. Sci.* **2008**, *97*, 3942–3956.
- (6) Caira, M. R. Sulfa Drugs As Model Cocrystal Formers. *Mol. Pharmaceutics* **2007**, *4*, 310–316.
- (7) Basavoju, S.; Bostrom, D.; Velaga, S. P. Indomethacin-Saccharin Cocrystal: Design, Synthesis and Preliminary Pharmaceutical Characterization. *Pharm. Res.* **2008**, *25*, 530–541.
- (8) Killinger, J. M.; Weintraub, H. S.; Fuller, B. L. Human Pharmacokinetic and Comparative Bioavailability of Loperamide Hydromacokinetic. *J. Clin. Pharmacol.* **1979**, *19*, 211–218.
- (9) Box K. J. Relationships between Lipophilicity and Solubility. Presented at: Physical Chemistry Symposium, November 29, 2006. <http://physchem.org.uk/symp02/symp02kb.pdf> (accessed December 2012).
- (10) Regnard, C.; Twycross, R.; Mihalyo, M.; Wilcock, A. Loperamide. *J. Pain Symptom Manage.* **2011**, *42*, 319–323.
- (11) Good, D. J.; Rodriguez-Hornedo, N. Solubility Advantage of Pharmaceutical Cocrystals. *Cryst Growth Des.* **2009**, *9*, 2252–2264.
- (12) Bruni, G.; Maietta, M.; Maggi, L.; Bini, M.; Capsoni, D.; Ferrari, S.; Boiocchi, M.; Berbenni, V.; Milanese, C.; Marini, A. Perphenazine–Fumaric Acid Salts with Improved Solubility: Preparation, Physico-Chemical Characterization and in Vitro Dissolution. *CrystEngComm* **2012**, *14*, 6035–6044.
- (13) Vogt, F. G.; Clawson, J. S.; Strohmeier, M.; Edwards, A. J.; Pham, T. N.; Watson, S. A. Solid State NMR Analysis of Organic Cocrystals and Complexes. *Cryst. Growth Des.* **2009**, *9*, 921–937.
- (14) Merrick, J. P.; Moran, D.; Radom, L. An Evaluation of Harmonic Vibrational Frequency Scale Factors. *J. Phys. Chem. A* **2007**, *111*, 11683–11700.



- (15) Wu, T.; Lin, S.-Y.; Huang, Y.-T. Simultaneous DSC-FTIR Microspectroscopy Used to Screen and Detect the Co-Crystal Formation in Real Time. *Biorg. Med. Chem. Lett.* **2012**, *21*, 3148–3151.
- (16) Antzutkin, O. N. Sideband Manipulation in Magic-Angle-Spinning Nuclear Magnetic Resonance. *Prog. Nucl. Magn. Reson. Spectrosc.* **1999**, *35*, 203–266.
- (17) Bruning, J.; Podgorski, D.; Alig, E.; Bats, J. W.; Schmidt, M. U. Antidiarrhetic Loperamide Hydro- Chloride. *Acta Crystallogr.* **2012**, *C68*, o111–o113.